

Original Article

Open Access



Sex differences in glutathione metabolism and acetaminophen toxicity

Allison Cruikshank¹ , Michael C. Reed¹, H. Frederik Nijhout² 

¹Department of Mathematics, Duke University, Durham, NC 27708, USA.

²Department of Biology, Duke University, Durham, NC 27708, USA.

Correspondence to: Prof. H. Frederik Nijhout. Department of Biology, Duke University, 130 Science Drive, Durham, NC 27708, USA. E-mail: hfn@gmail.com

How to cite this article: Cruikshank A, Reed MC, Nijhout HF. Sex differences in glutathione metabolism and acetaminophen toxicity. *Metab Target Organ Damage* 2024;4:17. <https://dx.doi.org/10.20517/mtod.2023.44>

Received: 16 Nov 2023 **First Decision:** 23 Feb 2024 **Revised:** 8 Mar 2024 **Accepted:** 26 Mar 2024 **Published:** 7 Apr 2024

Academic Editor: Amedeo Lonardo **Copy Editor:** Yanbing Bai **Production Editor:** Yanbing Bai

Abstract

Aims: Clinical and experimental evidence has shown that females in humans and other mammals have higher glutathione (GSH) levels than males, which are caused by higher levels of estradiol. Understanding how hepatic GSH level and synthesis velocity depend on the sex hormones is an extremely important question since oxidative stress contributes to the risk for heart disease and cancer, and oxidative stress is reduced by GSH. Our aim is to develop a systems approach to understanding GSH metabolism and use this to explain the causes of GSH differences in males and females, how GSH changes during the menstrual cycle, and why women may be less susceptible to acetaminophen toxicity.

Methods: We use mathematical models for hepatic glutathione metabolism, including one-carbon metabolism and acetaminophen detoxification, to investigate how the activation of certain enzymes by estradiol leads to dramatic changes in reaction velocities and metabolite concentrations.

Results: The models explain why women of childbearing age have higher glutathione than men, and that this is caused by the balance of activation of glutamyl cysteine synthetase (GCL) and glutathione peroxidase (GPX) by estradiol. The steady-state concentration of glutathione in women depends on the strength of the activation of GCL and GPX and is quite homeostatic over a wide range of activations.

Conclusions: During the menstrual cycle, the GSH concentration changes daily but over a relatively narrow range. We explain how this dynamic homeostasis depends on the biochemical network that produces GSH. The model is



© The Author(s) 2024. **Open Access** This article is licensed under a Creative Commons Attribution 4.0 International License (<https://creativecommons.org/licenses/by/4.0/>), which permits unrestricted use, sharing, adaptation, distribution and reproduction in any medium or format, for any purpose, even commercially, as long as you give appropriate credit to the original author(s) and the source, provide a link to the Creative Commons license, and indicate if changes were made.



also consistent with published results that show that female mice are less susceptible than males to hepatotoxicity due to acetaminophen overdose and suggests that this might also be true for humans, though the human epidemiological data are contradictory.

Keywords: Sex differences, glutathione, metabolism, liver, acetaminophen toxicity

INTRODUCTION

The tripeptide glutathione (GSH) is produced in prodigious quantities by the liver. It is the main antioxidant in the body and conjugates and eliminates a variety of toxicants, reactive oxygen species, and heavy metals. Glutathione is synthesized by a pathway that starts with homocysteine in the methionine cycle [Figure 1]. In the redox reaction catalyzed by glutathione peroxidase (GPX), GSH is converted to glutathione disulfide (GSSG), which can be reconverted to GSH by the enzyme glutathione reductase (GR).

Clinical and experimental evidence has accumulated that females in humans and other mammals have higher GSH levels than males, caused by higher levels of estradiol. In human females, blood GSH drops after ovariectomy from 54.69 to 39.29 nmol/L, but is restored by estrogen replacement therapy^[1]. Similar results have been obtained in rats^[2,3]. Adolescent girls have a higher GSH/GSSG ratio than males^[4]. Antioxidant gene expression is higher in females than in males and is accompanied by lower oxidative damage^[3]. In addition, there is considerable evidence that estrogen increases substantially the activities of GPX and Glutamate Cysteine Ligase (GCL), an enzyme in the GSH pathway^[5-7].

Understanding how GSH level and synthesis velocity depend on the sex hormones is an extremely important question since oxidative stress contributes to the risk for heart disease^[8] and cancer^[9], and oxidative stress is reduced by GSH via the enzyme GPX [Figure 1]. The pathways that regulate GSH production and recycling are extremely complex [Figure 1], and most research on this system has been conducted through association studies which can suggest local mechanisms but cannot fully capture the interactions in the system as a whole. In order to capture this complexity, we have, in collaboration with clinicians and experimentalists, developed mathematical models based on the real underlying physiology^[10-16]. These models are validated by their ability to reproduce a diversity of new experimental results, and can be used as platforms for in-silico experimentation to determine the underlying mechanisms that give rise to the behavior seen in the clinic and experiments. In this paper, we present a new integrated model for hepatic glutathione metabolism including one-carbon metabolism and use it to investigate how the activation of certain enzymes by estradiol in one-carbon metabolism and glutathione metabolism leads to dramatic changes in reaction velocities and metabolite concentrations, including GSH and the GSH synthesis rate. Since estradiol varies over a very wide range during the menstrual cycle, one might expect that GSH would show similar variability. In fact, we show that GSH shows homeostasis during the menstrual cycle and we explain the reason for this result.

GSH is connected to the hepatotoxicity of acetaminophen because it is used by the liver to bind a toxic byproduct (NAPQI) of acetaminophen metabolism. We study the effect of GSH and sexual dimorphism on acetaminophen toxicity by using a previously constructed model of acetaminophen metabolism^[10]. We show how the time curve of hepatic cell death depends on the dose of acetaminophen, and how it is affected by the timing of rescue by N-acetylcysteine. Experiments in mice show that female mice are much less sensitive to acetaminophen overdose^[17,18]. However, this question is controversial in humans^[19-21].

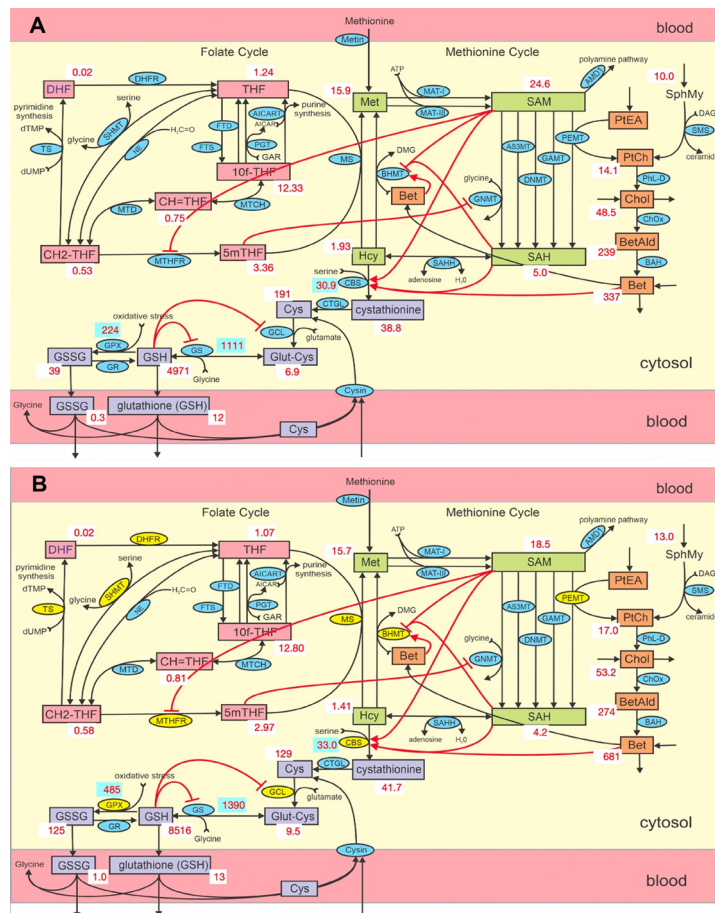


Figure 1. The male and female steady states. The rectangular boxes and ovals contain the acronyms of the substrates and enzymes, respectively. The yellow ovals in Panel B indicate enzymes whose activities differ between males and menstruating females. The white boxes indicate substrate values (μM) and the blue boxes indicate velocities ($\mu\text{M}/\text{hr}$). Panels A and B are the steady states for males and females, respectively. Full names of enzymes and substrates can be found in the supplementary material. As can be seen, the females have a much higher level of glutathione than males. The flux into the glutathione pathway (CBS) does not vary very much between males and females. So, the large difference in glutathione concentration must be because GCL and GPX are activated by estradiol.

METHODS

The mathematical models used in this paper were created by combining previous mathematical models and making a few adjustments. We have previously developed a mathematical model of sex differences and the effects of estradiol in one-carbon metabolism^[11,22]. To create the glutathione model used in this paper, we took the model from^[11] and added the glutathione pathway, homocysteine, cystathionine, cysteine, glutamylcysteine, GSH, and GSSG [Figure 1] from a previous model of glutathione metabolism^[14]. All of the velocities are given by Michaelis-Menten kinetics, with the K_m values taken from the literature, and where available, from human data. The adjustments are as follows: (1) For simplicity, we treat cytosolic serine and glycine as constant; (2) The male steady state is slightly different than in^[11], so we adjust the steady states of SAM, SAH, and Bet, which occur in the velocity equation for CBS and the velocity equation for BHMT; (3) We increased the V_{max} in the velocity equation for the transport of cysteine from the blood to the cytosol by a factor of 9; (4) We decreased the leakage rate of cytosolic cysteine from the cytosol to the blood from 1 to 0.25 h; (5) We multiplied the V_{max} of CTGL by 1/3.5; (6) We decreased the velocity for the transport of glutamate from other systems to the blood from 273 to 200 $\mu\text{M}/\text{hr}$. All of these velocities can be seen in Figure 1 and all of the abbreviations in the Table of Acronyms in the Supplementary materials.

Now, we discuss the activation of GCL and GPX by estradiol. There is a consensus that GPX and GCL are the two enzymes in the glutathione pathway that are upregulated by estradiol. Pinto and Bartley found 80% higher activity of GPX in female rats compared to males^[23]. Bellanti *et al.* studied human females and found that GPX mRNA was 134% higher in menstruating females than after ovariectomy^[1]. Wang *et al.* found that female rats had 80% higher GPX activity than females after maturity^[7]. For GCL, McConnachie *et al.* found somewhat less than a 100% increase in female mice^[17], and Dabrosin *et al.* found that estrogen causes an increase in GCL activity in human breast cells *in vitro*^[5]. Given these results, we decided to choose 80% as the “normal” or average increase in activity of GCL and GPX for females in our model for both of the enzymes GPX and GCL. Thus, we multiply the V_{max} values of GCL and GPX by a number, S , where $S = 1$ for males and $S = 1.8$ for females. In Section 3.2, we show that the steady-state concentration of GSH varies as S varies over a wide range, 1-3.5, but is fairly homeostatic near 1.8.

None of the studies cited above controlled for where the women or animals were during the menstrual (or estrus) cycle when the measurements were made. Nevertheless, by using our model, we can compute GSH during the entire human period of 28 days. We have good information on estradiol, $E_2(t)$, during the cycle; see Panel A of Figure 2. For women, $E_2(t)$, varies from 0.135 to 1.156 nM over the course of the cycle^[24,25], and for men, E_2 is a constant 0.09 nM^[26]. We assume that the function, $S(t)$, which multiplies the V_{max} values of GCL and GPX, is a linear function of $E_2(t)$ as follows:

$$(1) \quad S(t) = 1 + \frac{(0.8)}{0.4368 - 0.09} (E_2(t) - 0.09)$$

where 0.4368 is the average value of $E_2(t)$ during the cycle (calculated from Panel A of Figure 2). Thus, $S = 1$ for males, and for females, $S = 1.8$ for the average female E_2 , consistent with the 80% choice above. When we discuss the menstrual cycle in Section 3.3, $S(t)$ is given in terms of $E_2(t)$ by the formula (1). $E_2(t)$ itself is a piecewise linear function found by applying the spline function in Matlab to the data in Panel A of Figure 2 for estradiol as a function of day of the cycle for the average woman. For the enzymes affected by estradiol in one-carbon metabolism (yellow enzymes), as estradiol varies during the menstrual cycle, the multiplier of the V_{max} of the enzyme is scaled between the male value and the female value in table 3 in^[22].

In Section 3.4, we study the difference in response to acetaminophen (APAP) overdose in males and females after an overdose. To do this, we used a previous program to study whole-body acetaminophen metabolism^[10]. We run the GSH program and the APAP program together - they share the substrate GSH, which is drawn down by the overdose and replenished by the GSH synthesis pathway. The integrated code consists of 61 differential equations that are solved in Matlab. The GSH system has 31 differential equations for the substrate concentrations in the rectangular boxes in Figure 1. The schematic diagram for the acetaminophen part of the program can be seen in^[10], Figure 1. Full names of the substrates and enzymes are given in the Supplementary materials table of acronyms. Concentrations are in μM and velocities in $\mu\text{M}/\text{hr}$.

RESULTS

Sex differences in glutathione metabolism at steady state

We begin by comparing male and female differences in the model at steady state. Figure 1, Panel A and Figure 1, Panel B show the steady state for a male and a female, respectively. The rectangular boxes indicate substrates, and the blue or yellow ovals give the names of the enzymes catalyzing the reactions. A yellow oval in Panel B indicates that the enzyme is affected by estradiol and/or testosterone, and therefore, its activity is different in females than males. In folate and methionine metabolism, the increases or decreases of the enzymes in the yellow ovals are given in^[11]. In the Methods, we discussed why, based on experimental and clinical studies, we chose 80% as the increase in average activation of GCL and GPX by estradiol. Thus,

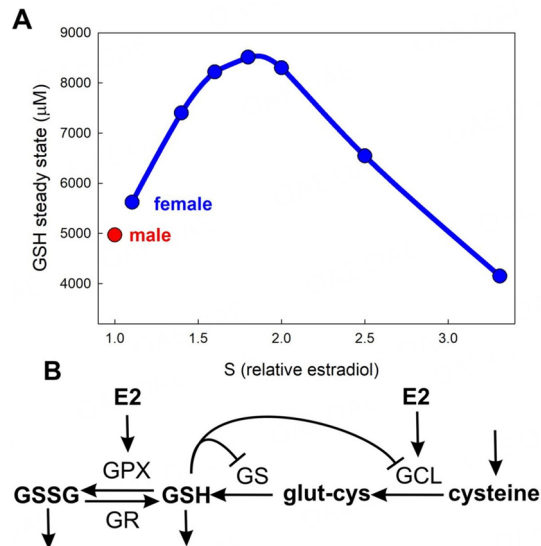


Figure 2. Consequences of the GSH regulatory motif. Panel B shows the GSH regulatory motif (taken from Figure 1), including the effects of estradiol and the inhibition of GCL and GS by GSH. Panel A shows the steady state value of GSH as a function of the parameter S , which increases with estradiol concentration and is defined in formula (2). The GSH curve goes up for low estradiol values, reaches a peak and descends for high estradiol values. The reasons for this behavior are discussed in the text.

the factor, S , multiplying the V_{max} values of GCL and GPX, will be $S = 1$ for males and $S = 1.8$ for females. The red arrows in Figure 1 show what we call “long-range interactions”, in which substrates allosterically affect distant enzymes in the network. There are even more allosteric interactions in the folate and the methionine cycles, but, for simplicity, we are not showing all of them. Note also that GSH inhibits both GCL and GS, so it is not clear by inspection of the diagram what the effect of raising the activities of GCL and GPX will be.

Panels A and B of Figure 1 show the steady state values for the male and female substrates, respectively, and the velocities for CBS, GS, and GPX. We will discuss several interesting aspects of the two figures. First, homocysteine (Hcy) is quite a bit lower in females than in males. The two reasons are that CBS is activated by estradiol and betaine (Bet), which is twice as high in females compared to males because the enzyme PEMT [Figure 1] is activated by a factor of 2.3 in menstruating females. This is not quite the whole story. The methionine input (in our model) is $40 \mu\text{M/hr}$, and if the mass leaving via the polyamine pathway (AMD1) is subtracted, the CBS flux is obtained because at steady state, the mass has nowhere else to go. Therefore, when CBS is activated by estradiol and betaine, the Hcy concentration must decrease to maintain the CBS flux at the correct level. Notice that CBS fluxes do not differ much between males and females, so this is not the reason that GSH differs so dramatically in males and females.

So, why is GSH so much higher in females than in males? The velocity of GS, the synthesizing enzyme, is not affected by estradiol. However, GCL is upregulated by estradiol, leading to a higher concentration of Glut-Cys in females, thereby driving increased GS flux. However, this is not the entire explanation, as estradiol also stimulates GPX, resulting in higher GPX flux that removes more mass from GSH. It is the balance between these two changes that determines the concentration of GSH [Table 1]. In this “average” female computation, GPX and GCL are upregulated by 80%. In the next section, we discuss the implications of stronger or weaker effects of estradiol.

Table 1. Steady state cellular concentrations (μM) and reaction velocities ($\mu\text{M}/\text{hr}$) as S varies. Notice that GSH goes up for low estradiol values, reaches a peak and descends for high estradiol values

S (relative estradiol)	1(male)	1.104	1.4	1.6	1.8	2	2.5	3.31
GSH	4,971	5,624	7,403	8,220	8,516	8,303	6,547	4,151
GSSG	38.91	47.5	76.9	100.4	125.5	150.6	203	248
bGSH	11.6	12.1	13.0	13.2	13.3	13.2	12.7	10.4
Velocity of GS	1,111	1,178	1,300	1,351	1,391	1,420	1,439	1,286
Velocity of GPX	448	520	724	853	970	1,070	1,244	1,367
Velocity of CBS	30.9	33.0	33.0	33.0	33.0	33.0	33.0	33.0

GSH: glutathione; GSSG: glutathione disulfide; bGSH: Plasma GSH; GPX: glutathione peroxidase; CBS: glutathione pathway.

Variation of GSH steady state depending on S

In our model, we take the activation of GCL and GPX by estradiol to be 80%, which is a reasonable choice supported by the experimental and clinical data discussed above. However, it is worth considering what would happen if we had chosen a different value, such as 60% or 100%. In the Methods, we explain why we take the multiplier, S , of the V_{max} values of GCL and GPX to have the following dependence on estradiol, E_2 :

$$(2) \quad S = 1 + \frac{(0.8)}{0.4368 - 0.09} (E_2 - 0.09)$$

Thus, since male E_2 is 0.09 nM^[26], $S = 1$ for the male. For the average female, E_2 varies from 0.135 to 1.156 nM during the menstrual cycle^[24,25]. Thus, for a female, the multiplier S will vary between 1.104 to 3.31 and $S = 1.8$ if $E_2 = 0.4368$ nM. This number, 0.4368 nM, is the average E_2 over the menstrual cycle computed from the data in Panel A of Figure 2. The steady state values of GSH and other variables for different values of S are shown in Table 1.

The concentrations of GSH in animal cells are in the range of 500-10,000 μM ^[27,28]. The ratio GSH/GSSG is thought to be around 100 for cells that are not under oxidative stress^[29], which aligns closely with the values presented in Table 1. Plasma GSH (bGSH) concentrations are typically measured in the range of 2-20 μM ^[28,30,31], consistent with the values in Table 1. Finally, as discussed in the previous section, we have elucidated why the velocity of CBS does not vary much between males and females.

The most interesting aspect of the data in Table 1 is the non-monotone behavior of GSH as S increases from 1 to 3.31 [Figure 2A]. S is calculated from estradiol by formula (2). In the lower range of values of S , GSH increases rapidly as S increases. GSH reaches a maximum at $S = 1.8$ (8,516 μM) and then descends to 4,151 μM for $S = 3.31$. This effect arises because of the nonlinear inhibition of GCL and GS by GSH [Figure 2B]. This is a kind of end-product inhibition that prevents the GSH concentration from rising too high. To understand the non-monotone behavior of GSH, it is crucial to consider that there are two incoming fluxes to GSH, GS and GR, and two outgoing fluxes, GPX and a large flux out into the blood [Figure 2B]. At a steady state, the incoming fluxes must balance the outgoing fluxes. When S is low, 1-1.4, the GS flux rises more rapidly than the GPX flux, pushing GSH up. Around $S = 1.4$, the GS flux starts to increase more slowly while the GPX flux still increases at roughly the same rate as S increases, so the GSH curve starts to level off and reaches a maximum at $S = 1.8$. After that, the increase in the GPX flux dominates as the GS flux increases more and more slowly and eventually declines. This behavior of the GS flux is caused by the competition between the higher inhibition of GS and GCL by GSH and the higher stimulation of GCL by estradiol [Figure 2].

The steady-state concentration of GSH remains relatively stable between $S = 1.4$ and $S = 2$, corresponding to increases in stimulation ranging from 40% to 100% compared to males. Therefore, we could have chosen any percentage within the 40% to 100% range to represent the average estradiol in females. We opted for an 80% increase in stimulation based on the consensus reached in several experimental studies conducted on rats and mice^[7,17,23]. It is natural to speculate whether the inhibition of GS and GCL is an important evolutionary mechanism to keep GSH high, but not too high, in females during the childbearing years.

The stability of GSH during the menstrual cycle

Since we know how estradiol varies during the menstrual cycle (Figure 3, Panel A), formula (1) provides insights into the value of the multiplier, S , for every day. It might seem intuitive, albeit incorrect, to calculate GSH levels over the cycle by calculating the steady-state GSH for each day of the cycle. This calculation would suggest that GSH levels vary between all the steady state values ranging from 4,151 to 8,516 μM [Table 1 and Figure 2A]. However, this prediction is inaccurate; actual GSH values fluctuate within a much narrower range, as illustrated in Panel B of Figure 3.

We compute GSH during the cycle as follows. Starting at any initial values, we use our GSH program to compute GSH(t) for 20×28 days, i.e., for twenty 28-day months. For the first few months (approximately 6), the solution is not periodic but gets closer and closer to a periodic function. During the 19th month, the solution is the same as that of the 20th month, indicating that the solution during the 20th month represents GSH(t) during the menstrual cycle. The periodic solution in Panel B of Figure 3, GSH(t), is quite stable, fluctuating only between 5,500 and 8,000 μM (even though the steady state values vary between 4,151 and 8,516 μM). We verified this calculation in two ways. Firstly, we confirmed that the solution during the 19th month (and indeed for many earlier months) matches that of the 20th month. Secondly, by initiating the program with many different initial conditions, we consistently arrived at the same periodic solution after a few months.

The intuitive reason that GSH(t) is fairly stable is that GSH changes quite slowly when estradiol and $S(t)$ vary. Table 2 shows an example. We began with the steady state for $S = 1.8$, but changed the value of S to 1.3 at $t = 0$, where the steady state of GSH is 6,842 μM . Table 2 shows the h and days as GSH slowly descends to 6,842 μM . The transition takes about 28 days.

Because GSH changes very slowly when estradiol and S change, the GSH concentration at each time is a weighted average of both low and high GSH concentrations corresponding to many different S values; this is the reason why GSH is so homeostatic. Note that the only significant deviation of GSH in Panel B of Figure 2 occurs during days 10-14 when estradiol and S become very high, thus depressing the GSH concentration [Table 1].

Sex differences in the toxicity of acetaminophen

Acetaminophen (APAP) is the most widely used over-the-counter and prescription painkiller in the world^[32]. While safe at therapeutic doses of up to 4 g per day for adults, APAP overdoses, either accidental or intentional, are one of the leading causes of acute liver failure in the United States^[33]. APAP is metabolized by conjugation with sulfate and glucuronidate; these conjugates are inert and are excreted in the urine. Depending on the dose, a fraction of APAP is converted into a highly reactive toxic intermediate, N-acetyl-p-benzoquinone imine (NAPQI), by several P450 cytochromes^[34]. Substantial amounts of NAPQI are effectively eliminated by conjugation with glutathione (GSH). However, after a large dose of APAP, the sulfonation reaction becomes saturated and the build-up of NAPQI depletes GSH in the liver, causing further accumulation of NAPQI. Unconjugated NAPQI binds to proteins and subcellular structures and induces rapid cell death and necrosis that can lead to liver failure.

Table 2. GSH (μM) changes slowly after S switches from $S = 1.8$ to $S = 1.3$. This is the reason that GSH varies less in the menstrual cycle than the steady states of GSH would suggest

Time	0 h	10 h	1 day	2 days	5 days	14 days	28 days
GSH	8,516	8,162	7,945	7,691	7,230	6,877	6,843

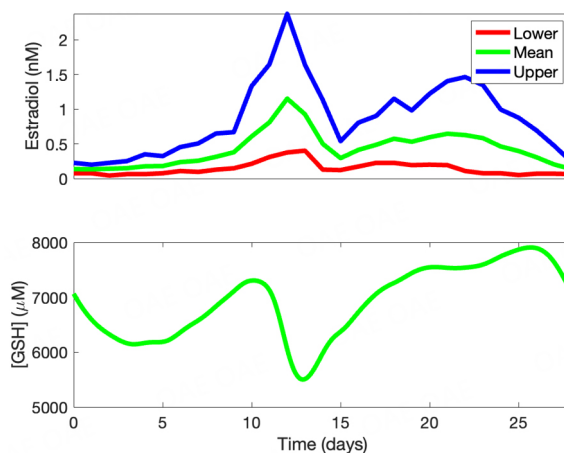


Figure 3. The stability of GSH. Panel A shows the 95th percentile (blue), the mean (green), and the 5th percentile (red) of estradiol during the menstrual cycle. The curves are drawn by interpolation of data from^[24,25]. Panel B shows the relative stability of GSH during the cycle (varying from 5,500 to 7,900 μM). This is true despite the wide range of steady state values [Table 1 and Figure 2A]. See the text for an explanation.

Many experimental studies have shown that female mice are less susceptible to APAP hepatotoxicity than males and that the sex differences are substantial^[17,18,35]. Many of the mechanisms have been elucidated by the Jaeschke group in Kansas^[18,36,37]. Here, we combine our APAP model^[10] with the one-carbon and glutathione model described in Methods. We show that, indeed, the sex differences are substantial, and we give an explanation. Our APAP model is a whole-body model of APAP that includes transport from the gut to the liver, the liver metabolism described in the previous paragraph, transport out of the liver to the blood, and excretion in the urine. The physiological basis of our model is the reaction diagram [Figure 1] and the K_m values for the enzymes; we choose human values when they are available. We choose compartment sizes and doses corresponding to humans. It should be noted that we do not include mitochondrial glutathione, which the Jaeschke group has found to be fundamental in APAP pathophysiology^[36]. To replicate specific mitochondrial GSH mechanisms and data from *in vivo* mice models, a mitochondrial compartment needs to be added. Nonetheless, our modeling study^[10] showed that the model results compare well to several experimental and clinical studies (figure 2, figure 6, figure 13 in^[10]). In particular, we showed that our predictions of life and death after overdose correspond well to a clinical study in the University of Utah Hospital; see figure 13 in^[10]. Our APAP model, combined with our GSH model, gives predictions about humans.

The epidemiological data on sex differences in acetaminophen-induced liver injury in humans is inconsistent, which can be attributed to confounding factors such as variations in age, dosage, time elapsed from ingestion to hospitalization, and time from ingestion to N-acetylcysteine administration. For example, in a United States retrospective study^[20], it was found that women have a higher risk of adverse outcomes than men in cases of acetaminophen-induced acute liver injury. However, a prospective study in Iceland^[19] reported that the prevalence of hepatotoxicity was higher in men than in women. In this same study, older age, not sex, was associated with the risk of acute liver failure. Another population-based study done in

Asia^[21] found a significant association of hepatotoxicity with ethnicity, while it found no such association with sex or age.

The maximal therapeutic dose recommended by the FDA is 4 g/day. With this therapeutic dose, there is little cell death and little change in GSH for both males and females. A 20 g dose without treatment is considered possibly lethal^[38]. It is important to note that there is variability among human clinical data and our model only makes predictions for the “average” human. We have found that the greatest differences between the male and female responses are in the moderate to high range, which is why we show responses to 15 and 18 g in [Figure 4](#). A very high dose of 30 g shows little difference between males and females.

In [Figure 4](#), we show the percentage of healthy liver cells still alive and the GSH concentration in the liver for the male and for the female for the first 80 h after ingestion of an overdose. Panels A, B, and C show the percentage of surviving hepatocytes for a 15 g dose, for an 18 g dose, and for a 30 g dose for males and females, respectively. The grey bar represents the 30% level of functional hepatocytes below which liver failure is thought to occur^[38]. In Panel A, one can see that the 15 g dose has a relatively small effect on the percentage of surviving hepatocytes in females, descending only from 1 to 0.9. In males, by contrast, the percentage declines below 0.4, dangerously close to the 0.3 survival line. Panels D, E, and F show that GSH levels plunge to near zero in all cases, but that GSH recovers more rapidly in females. Panel B shows the time course of functional hepatocytes after an 18 g dose of APAP. In this case, the female curve descends below 0.6 and the male curve descends well below 0.3. Therefore, without treatment, the female is predicted to live, and the male is predicted to die. Again, we see in Panel E that female GSH recovers more quickly than male GSH. This reproduces a result found by Du *et al.*^[18]. With the 30 g dose, both males and females die and there is not much difference between the curves^[37]. These are the results of APAP overdose without treatment; we consider intervention in the next section.

Our computations show that the sexual dimorphism in one-carbon metabolism plays only a small role in the glutathione pathway (the velocity of CBS is not much different in the two cases, [Table 1](#)). So, it is the estradiol and the regulatory motif ([Figure 2](#), Panel B) that increases the synthesis velocity and the concentration of GSH in the female liver.

GSH is a tripeptide consisting of glutamate, glycine, and cysteine. Of the three, cysteine has a far lower concentration in liver cells than glutamate and glycine. Thus, intravenous N-acetylcysteine (NAC) is the antidote for APAP overdose given in Emergency Departments. NAC limits the hepatotoxicity of APAP by increasing the synthesis of GSH in the liver^[39]. Our APAP program allows us to investigate the consequences of different dosing protocols of NAC on the recovery of GSH after an APAP overdose^[10]. We illustrate this by attempting to rescue the male [[Figure 5](#)] after an 18 g overdose of APAP. A typical dose of NAC is 300 mg/kg, which is approximately 18 gm for a 60 kg person, or 36,000 μM of NAC. We give 1/3 of this dose over the first 2 h and 2/3 of this dose over the next 3 h. The results are shown in [Figure 5](#).

The black curve in [Figure 5](#) shows the response of the male to an 18-gm dose of APAP if not treated. The result is almost certain liver failure because he has less than 30% of his hepatocytes over an extended time. The green curve shows the rescue of the male by the protocol described above, starting 10 h after ingestion. Since the green curve stays above the 30% line, the man will likely survive. The pink curve shows rescue by NAC starting at 16 h after ingestion. Rescue is possible but problematic since the pink curve descends somewhat below 30%. The contrasting outcomes of rescue at 10 h vs. 16 h underscore the widely acknowledged clinical observation that early intervention is crucial^[40,41]. It is important to highlight the variability of clinical data; for instance, case reports have demonstrated survival after a 25 g overdose^[42], and

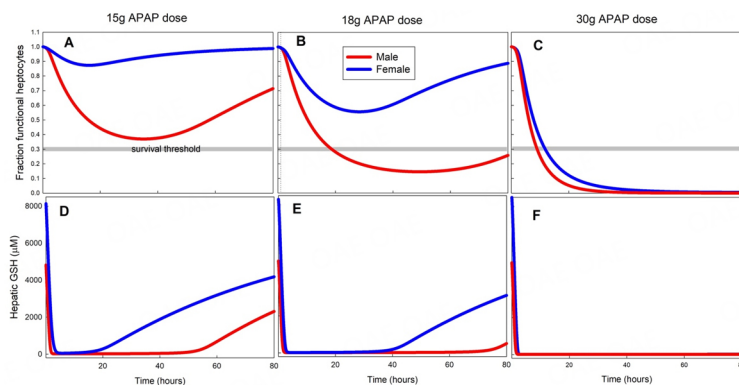


Figure 4. Sexual differences in responses to APAP. Panels A, B, and C show the percentage of surviving hepatocytes for females (blue curves) and males (red curves) for a 15 g dose, an 18 g dose of APAP, and a 30 g dose of APAP, respectively, over the first 80 h after ingestion. The 15 g dose is not lethal, the 18 g dose is marginally lethal, and the 30 g dose is definitely lethal without NAC rescue in the ER. The 15 g and 18 g doses show large differences between males and females, while at 30 g, the responses are similar. At 4 g, the daily maximal dose recommended by the FDA, there is also no difference between the sexes (simulations not shown). Panels D, E, and F show the corresponding concentration curves for GSH. As shown in the literature^[18], for moderate to high doses, female GSH recovers more quickly than male GSH.

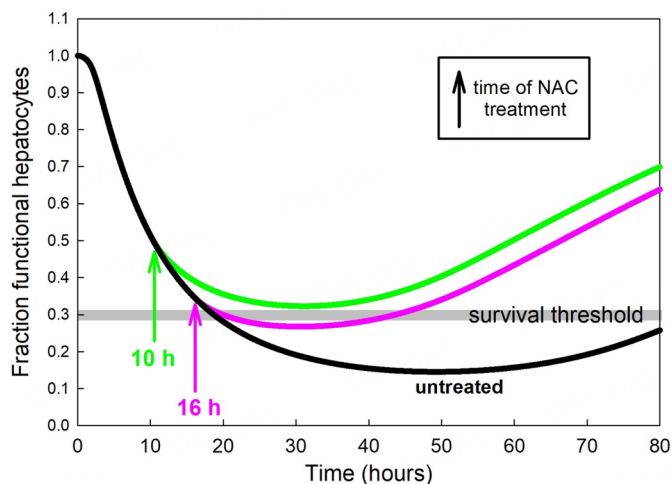


Figure 5. Rescue by N-acetyl Cysteine. The black curve shows the response of the male to an 18-gm dose of APAP if not treated. The result is almost certain liver failure. The green curve shows the NAC rescue of the male by the protocol described in the text starting 10 h after ingestion. The pink curve shows rescue by NAC starting at 16 h after ingestion; rescue is possible but problematic.

current guidelines in the United States and Canada indicate a high-risk ingestion to be ingestion of at least 30 g of APAP^[43].

DISCUSSION

By combining previous models and making a few parameter changes, we have created a new model of glutathione metabolism that we have used to investigate sexual dimorphism in the glutathione pathway in the liver. Although many enzymes in one-carbon metabolism are affected by the sex hormones testosterone and estradiol, the main reasons for sexual dimorphism in glutathione metabolism are the effects of estradiol and the GSH regulatory motif, which includes the inhibition of GS and GCL by GSH itself [Figure 2B]. To understand the effects of estradiol on such a complicated network, mathematical computation is required.

We defined S to be a factor multiplying the V_{max} values of GCL and GPX representing the activation of GCL and GPX, so $S = 1$ for males and $S = 1.8$ for females for average estradiol, since we make a case based on experimental and clinical results that the activation is by 80%. Then, we showed in [Figure 1](#) that the male steady-state concentration of GSH is 4,971 μM , while the female steady-state concentration of GSH is 8,516 μM . In addition, the rate of synthesis of GSH, GS, is higher in females. In Section 2, we computed how the steady-state concentration of GSH in females depends on the size of S . Interestingly, the female steady-state is low for S near 1 and also low for $S = 3.31$, but at intermediate values of S , the female steady-state is considerably higher than that the male's. We explained that this non-monotone behavior of the female GSH curve is caused by the inhibition of GCL and GS by GSH.

GSH is the main antioxidant and detoxicant in the body. Using a previous model^[10], we explained how this works in the case of acetaminophen (APAP) which is hepatotoxic. Our model suggests that the large male-female differences in GSH concentration and the velocity of its synthesis cause females to be less sensitive to APAP toxicity compared to males. This is consistent with experimental data in mice^[17,18] and in the human study^[19]. We note, however, that human studies are controversial on this point.

We also investigated the behavior of GSH(t) during the menstrual cycle, and showed that GSH remains stable during the menstrual cycle, which was completely unexpected given the wide range of GSH steady states seen in [Figure 2](#). We explained that this important result arises from the very slow change of GSH as $S(t)$ is varied, and suggest that this may be an important evolutionary adaptation.

LIMITATIONS

Our models are based on the underlying physiology and the kinetics of the enzymes, but no model can encompass the entirety of biological complexity. Thus, our model necessarily incorporates simplifications. In our model, serine and glycine in the cell remain constant, as is methionine input (important for the synthesis of cysteine). For simplicity, we assume that the activations of GCL and GPX are equal, though that may not be the case. There is a lot of variance in gene expression levels, even for identical genes in different individuals^[44-46]. The amount of estradiol produced during the menstrual cycle varies a lot in different women (see Panel A of [Figure 3](#)). Our APAP model^[10] is simple because it does not include the processing of GSH in the mitochondria that has been shown to be fundamental for liver cell death in the presence of APAP^[36]. We also take 30% of surviving hepatocytes to be the boundary between surviving and dying without NAC rescue^[38]. Human responses are variable, and the outcomes may depend on the overall health of the patient. In fact, it has been reported that some mice die even though they retain 70% of their hepatocytes^[37]. Finally, we have concentrated on the effect of estradiol on glutathione metabolism and have not included the effects of progesterone^[47-49].

DECLARATIONS

Authors' contributions

Developed the model, ran simulations and analyses, interpreted the findings, and contributed to the writing and editing of the manuscript: Cruikshank A, Reed MC, Nijhout HF

Availability of data and materials

Computer models and codes used in this paper can be obtained from the authors by request.

Financial support and sponsorship

This work was supported by grants from the National Science Foundation (<https://www.nsf.gov/>); IOS-1557341 (HFN, MCR) and DMS-2038056 (AC); and the National Institute of Health (<https://www.nih.gov/>); 1R01MH106563-01A1 (HFN, MCR).

The funders had no role in study design, data collection and analysis, decision to publish, or preparation of the manuscript.

Conflicts of interest

All authors declared that there are no conflicts of interest.

Ethical approval and consent to participate

Not applicable.

Consent for publication

Not applicable.

Copyright

© The Author(s) 2024.

REFERENCES

1. Bellanti F, Matteo M, Rollo T, et al. Sex hormones modulate circulating antioxidant enzymes: impact of estrogen therapy. *Redox Biol* 2013;1:340-6. DOI PubMed PMC
2. Abbas AM, Elsamanoudy AZ. Effects of 17 β -estradiol and antioxidant administration on oxidative stress and insulin resistance in ovariectomized rats. *Can J Physiol Pharmacol* 2011;89:497-504. DOI PubMed
3. Borrás C, Sastre J, García-Sala D, Lloret A, Pallardó FV, Viña J. Mitochondria from females exhibit higher antioxidant gene expression and lower oxidative damage than males. *Free Radic Biol Med* 2003;34:546-52. DOI PubMed
4. de Toda I, González-Sánchez M, Díaz-Del Cerro E, Valera G, Carracedo J, Guerra-Pérez N. Sex differences in markers of oxidation and inflammation. Implications for ageing. *Mech Ageing Dev* 2023;211:111797. DOI PubMed
5. Dabrosin C, Ollinger K. Variability of glutathione during the menstrual cycle-due to estrogen effects on hepatocytes? *Free Radic Biol Med* 2004;36:145-51. DOI PubMed
6. Ha EJ, Smith AM. Plasma selenium and plasma and erythrocyte glutathione peroxidase activity increase with estrogen during the menstrual cycle. *J Am Coll Nutr* 2003;22:43-51. DOI PubMed
7. Wang L, Ahn YJ, Asmis R. Sexual dimorphism in glutathione metabolism and glutathione-dependent responses. *Redox Biol* 2020;31:101410. DOI PubMed PMC
8. Salonen JT, Alftan G, Huttunen JK, Pikkarainen J, Puska P. Association between cardiovascular death and myocardial infarction and serum selenium in a matched-pair longitudinal study. *Lancet* 1982;2:175-9. DOI
9. Combs GF Jr, Gray WP. Chemopreventive agents: selenium. *Pharmacol Ther* 1998;79:179-92. DOI PubMed
10. Ben-Shachar R, Chen Y, Luo S, Hartman C, Reed M, Nijhout HF. The biochemistry of acetaminophen hepatotoxicity and rescue: a mathematical model. *Theor Biol Med Model* 2012;9:55. DOI PubMed PMC
11. Kim R, Nijhout HF, Reed MC. One-carbon metabolism during the menstrual cycle and pregnancy. *PLoS Comput Biol* 2021;17:e1009708. DOI PubMed PMC
12. Nijhout HF, Reed MC, Anderson DF, Mattingly JC, James SJ, Ulrich CM. Long-range allosteric interactions between the folate and methionine cycles stabilize DNA methylation reaction rate. *Epigenetics* 2006;1:81-7. DOI PubMed
13. Nijhout HF, Reed MC, Budu P, Ulrich CM. A mathematical model of the folate cycle: new insights into folate homeostasis. *J Biol Chem* 2004;279:55008-16. DOI PubMed
14. Reed MC, Thomas RL, Pavisic J, James SJ, Ulrich CM, Nijhout HF. A mathematical model of glutathione metabolism. *Theor Biol Med Model* 2008;5:8. DOI PubMed PMC
15. Reed MC, Lieb A, Nijhout HF. The biological significance of substrate inhibition: a mechanism with diverse functions. *Bioessays* 2010;32:422-9. DOI PubMed
16. Thanacoody H, Nijhout H, Reed M, Thomas C. Mathematical modelling of the effect of a high dose acetylcysteine regimen based on the SNAP trial on hepatic glutathione regeneration and hepatocyte death. Available from: <https://www.tandfonline.com/doi/epdf/10.3109/15563650.2016.1165952?needAccess=true> [Last accessed on 8 Apr 2024].
17. McConnachie LA, Mohar I, Hudson FN, et al. Glutamate cysteine ligase modifier subunit deficiency and gender as determinants of acetaminophen-induced hepatotoxicity in mice. *Toxicol Sci* 2007;99:628-36. DOI
18. Du K, Williams CD, McGill MR, Jaeschke H. Lower susceptibility of female mice to acetaminophen hepatotoxicity: role of mitochondrial glutathione, oxidant stress and c-jun N-terminal kinase. *Toxicol Appl Pharmacol* 2014;281:58-66. DOI PubMed PMC
19. Björnsson ES, Bergmann OM, Björnsson HK, Kvaran RB, Olafsson S. Incidence, presentation, and outcomes in patients with drug-induced liver injury in the general population of Iceland. *Gastroenterology* 2013;144:1419-25, 1425.e1-3; quiz e19-20. DOI PubMed
20. Rubin J, Hameed B, Gottfried M, Lee W, Sarkar M. Sex differences in acetaminophen-induced acute liver injury and acute liver

- failure. *J Hepatol* 2016;64:S173-4. DOI
21. Marzilawati AR, Ngau YY, Mahadeva S. Low rates of hepatotoxicity among Asian patients with paracetamol overdose: a review of 1024 cases. *BMC Pharmacol Toxicol* 2012;13:8. DOI PubMed PMC
 22. Sadre-Marandi F, Dahdouh T, Reed MC, Nijhout HF. Sex differences in hepatic one-carbon metabolism. *BMC Syst Biol* 2018;12:89. DOI PubMed PMC
 23. Pinto RE, Bartley W. The effect of age and sex on glutathione reductase and glutathione peroxidase activities and on aerobic glutathione oxidation in rat liver homogenates. *Biochem J* 1969;112:109-15. DOI PubMed PMC
 24. Sluss PM, Hayes FJ, Adams JM, et al. Mass spectrometric and physiological validation of a sensitive, automated, direct immunoassay for serum estradiol using the architect. *Clin Chim Acta* 2008;388:99-105. DOI
 25. Stricker R, Eberhart R, Chevailler MC, Quinn FA, Bischof P, Stricker R. Establishment of detailed reference values for luteinizing hormone, follicle stimulating hormone, estradiol, and progesterone during different phases of the menstrual cycle on the Abbott ARCHITECT analyzer. *Clin Chem Lab Med* 2006;44:883-7. DOI PubMed
 26. Cooke PS, Nanjappa MK, Ko C, Prins GS, Hess RA. Estrogens in male physiology. *Physiol Rev* 2017;97:995-1043. DOI PubMed PMC
 27. Inoue M, Kinne R, Tran T, Arias IM. Glutathione transport across hepatocyte plasma membranes. Analysis using isolated rat-liver sinusoidal-membrane vesicles. *Eur J Biochem* 1984;138:491-5. DOI PubMed
 28. Wu G, Lupton JR, Turner ND, Fang YZ, Yang S. Glutathione metabolism and its implications for health. *J Nutr* 2004;134:489-92. DOI
 29. Griffith OW. Biologic and pharmacologic regulation of mammalian glutathione synthesis. *Free Radic Biol Med* 1999;27:922-35. DOI PubMed
 30. James SJ, Cutler P, Melnyk S, et al. Metabolic biomarkers of increased oxidative stress and impaired methylation capacity in children with autism. *Am J Clin Nutr* 2004;80:1611-7. DOI
 31. Pogribna M, Melnyk S, Pogribny I, Chango A, Yi P, James SJ. Homocysteine metabolism in children with Down syndrome: in vitro modulation. *Am J Hum Genet* 2001;69:88-95. DOI PubMed PMC
 32. Daly FF, Fountain JS, Murray L, Graudins A, Buckley NA; Panel of Australian and New Zealand clinical toxicologists. Guidelines for the management of paracetamol poisoning in Australia and New Zealand—explanation and elaboration. A consensus statement from clinical toxicologists consulting to the Australasian poisons information centres. *Med J Aust* 2008;188:296-301. DOI PubMed
 33. Lee WM. Acetaminophen-related acute liver failure in the United States. *Hepatol Res* 2008;38 Suppl 1:S3-8. DOI PubMed
 34. Prescott LF. Kinetics and metabolism of paracetamol and phenacetin. *Br J Clin Pharmacol* 1980;10 Suppl 2:291S-8S. DOI PubMed PMC
 35. Masubuchi Y, Nakayama J, Watanabe Y. Sex difference in susceptibility to acetaminophen hepatotoxicity is reversed by buthionine sulfoximine. *Toxicology* 2011;287:54-60. DOI PubMed
 36. Ramachandran A, Jaeschke H. Mitochondria in acetaminophen-induced liver injury and recovery: a concise review. *Livers* 2023;3:219-31. DOI PubMed PMC
 37. Nguyen NT, Umbaugh DS, Smith S, et al. Dose-dependent pleiotropic role of neutrophils during acetaminophen-induced liver injury in male and female mice. *Arch Toxicol* 2023;97:1397-412. DOI PubMed PMC
 38. Remien CH, Adler FR, Waddoups L, Box TD, Sussman NL. Mathematical modeling of liver injury and dysfunction after acetaminophen overdose: early discrimination between survival and death. *Hepatology* 2012;56:727-34. DOI PubMed
 39. Schilling A, Corey R, Leonard M, Eghtesad B. Acetaminophen: old drug, new warnings. *Cleve Clin J Med* 2010;77:19-27. DOI
 40. Prescott LF, Illingworth RN, Critchley JA, Stewart MJ, Adam RD, Proudfoot AT. Intravenous N-acetylcysteine: the treatment of choice for paracetamol poisoning. *Br Med J* 1979;2:1097-100. DOI PubMed PMC
 41. Smilkstein MJ, Knapp GL, Kulig KW, Rumack BH. Efficacy of oral N-acetylcysteine in the treatment of acetaminophen overdose. Analysis of the national multicenter study (1976 to 1985). *N Engl J Med* 1988;319:1557-62. DOI PubMed
 42. Link SL, Rampon G, Osmon S, Scalzo AJ, Rumack BH. Fomepizole as an adjunct in acetylcysteine treated acetaminophen overdose patients: a case series. *Clin Toxicol* 2022;60:472-7. DOI
 43. Dart RC, Mullins ME, Matoushek T, et al. Management of acetaminophen poisoning in the US and Canada: a consensus statement. *JAMA Netw Open* 2023;6:e2327739. DOI
 44. Boeuf S, Keijer J, Franssen-Van Hal NL, Klaus S. Individual variation of adipose gene expression and identification of covariated genes by cDNA microarrays. *Physiol Genomics* 2002;11:31-6. DOI PubMed
 45. Oleksiak MF, Churchill GA, Crawford DL. Variation in gene expression within and among natural populations. *Nat Genet* 2002;32:261-6. DOI PubMed
 46. Sigal A, Milo R, Cohen A, et al. Variability and memory of protein levels in human cells. *Nature* 2006;444:643-6. DOI PubMed
 47. Itagaki T, Shimizu I, Cheng X, et al. Opposing effects of oestradiol and progesterone on intracellular pathways and activation processes in the oxidative stress induced activation of cultured rat hepatic stellate cells. *Gut* 2005;54:1782-9. DOI PubMed PMC
 48. Yuan XH, Fan YY, Yang CR, et al. Progesterone amplifies oxidative stress signal and promotes NO production via H₂O₂ in mouse kidney arterial endothelial cells. *J Steroid Biochem Mol Biol* 2016;155:104-11. DOI
 49. Ohwada M, Suzuki M, Sato I, Tsukamoto H, Watanabe K. Glutathione peroxidase activity in endometrium: effects of sex hormones and cancer. *Gynecol Oncol* 1996;60:277-82. DOI PubMed